

Polyvinyl-alcohol fiber–reinforced concrete with coarse aggregate in beam elements

Leonardo M. Massone*, Jaime Reveco, Alejandro Arenas and Fabián Rojas

University of Chile, Department of Civil Engineering, Blanco Encalada 2002, Santiago, Chile

(Received November 30, 2022, Revised March 11, 2023, Accepted March 23, 2023)

Abstract. The use of fibers has been commonly considered in engineered cementitious composites, but their behavior with coarse aggregate in concrete has not been studied significantly, which is needed to meet structural performance objectives for design, such as ductility. This research analyzes the behavior of fiber-reinforced concrete with coarse aggregate with 0.62%, 1.23%, and 2% PVA (Polyvinyl-alcohol) content, varying the maximum aggregate size. Tensile (direct and indirect) and compressive concrete tests were performed. The PVA fiber addition in coarse aggregate concrete increased the ductility in compression, especially for the fiber with a larger aspect ratio, with a minor impact on strength. In addition, the tensile tests showed that the PVA fiber increased the tensile strength of concrete with coarse aggregate and, more significantly, improved the ductility. A selected mixture was used to build short and slender reinforced concrete beams to assess the behavior of structural members. PVA fiber addition in short beams changed the failure mode from shear to flexure, increasing the deflection capacity. On the other hand, the slender beam tests revealed negligible impact with the use of PVA.

Keywords: beam; coarse aggregate; compression; fiber–reinforced; Polyvinyl-alcohol; PVA; tension

1. Introduction

Concrete is a material made from a mixture of cement, sand, gravel, water, and other aggregates, such as accelerants and retardant additives. Its primary constitutive materials—sand, gravel, and water—are usually available at a low cost near the construction site. Concrete has a high compression strength, which makes it suitable for casting members subjected primarily to compressions. However, as a mixture of fine and coarse particles, concrete is a relatively brittle material whose tensile strength is low compared with its compressive strength. Thus, concrete is commonly reinforced with steel or plastic fibers (fiber-reinforced concrete; FRC) or steel bars (reinforced concrete; RC) to support tensile stresses, often present in shear and flexural behavior (Kang *et al.* 2012), for applications including frames, pavement, and tunnels (Massone and Nazar 2018). Current design performance objectives require knowledge of failure modes of structural elements and systems, as well as deformation or ductility capacity (Massone 2013, Massone *et al.* 2023), such that the structural behavior can be enhanced in the design process with the use of fibers.

The durability and cost of steel fibers (Brandt 2008) are the main concerns when considering

*Corresponding author, Professor, E-mail: lmassone@uchile.cl

them as suitable reinforcements for structural applications (Khan and Ayub 2016). The use of PVA (polyvinyl-alcohol) fibers has an advantage over steel fibers in the slip-hardening response (Holschemacher and Höer 2008), they resist corrosion, cost less because of the lower density and the development of new material formulations (Karimpour and Mazloom 2022), and require less cement compared to the same volume of steel fibers. PVA is manufactured by the polymerization of vinyl acetate monomer into polyvinyl acetate (PVAc), followed by the hydrolysis of the acetate groups of PVAc to PVA (Thong *et al.* 2016). It is non-hazardous, safe to handle, and environmentally friendly. This fiber presents suitable characteristics in an FRC as it has high strength and elastic modulus compared to other fibers, such as polypropylene, nylon, and polyethylene.

PVA fibers like steel and glass fibers are the most promising in tensile strength, elastic modulus, and fiber elongation. In comparison to other synthetic fibers, PVA fibers have demonstrated stronger bonds with the cement matrix compared to others (Horikoshi *et al.* 2006). Therefore, PVA fibers have been widely used in engineered cementitious composites (ECCs) (e.g., Yu *et al.* 2018), which have limited structural applications for the lack of coarse aggregates (Li *et al.* 1998). The influences of fiber type, length, and volume, among other factors, have been studied extensively for ECCs with small aggregate size (e.g., Cao *et al.* 2019). High aggregate content and the presence of coarse aggregates in a paste tend to increase the matrix toughness, which delays crack initiation and prevents steady-state flat-crack propagation, resulting in a loss of the tensile ductility of ECC (Sahmaran *et al.* 2012). Typical maximum particle gradations diameters used in most FRC investigations with ECC are smaller than 0.5 mm (Aghdasi *et al.* 2016). Because of the negative interaction between the fiber and cementitious particles, a larger particle yields a bigger air-void content inside the matrix, leading to a diminished specimen strength (Sahmaran *et al.* 2012). Alyousif *et al.* (2016) presented test results for RC beam specimens with normal and ECC concrete modified with PVA. The results for beams with a ratio of shear span a to effective depth d (a/d) varying from 1 to 3 showed that the ductility was low for normal concrete compared to that of the ECC specimens. In this testing, shear failure was promoted because of the absence of stirrups, whereas the specimens with PVA fibers in the ECC modified the shear failure to a more ductile flexural failure. Push-off tests for shear characterization have also shown the shear improvement with the addition of PVA fibers (Georgiou and Pantazopoulou 2019). Similar results were obtained for slender beams ($a/d = 4$) with stirrups, but in this case, the use of ECC in the compressive zone of the beams improved the response considerably, whereas when ECC was included in the tensile zone of beams, the impact was smaller (Batan *et al.* 2021). In shorter beams ($a/d = 2.6$), also with stirrups, the addition of PVA fibers (2%) in the entire specimen improved the strength and ductility by about 30% and 60%, respectively, however, when PVA was added only to the tensile zone, the improvement in ductility was less significant (Shanour *et al.* 2018). Other cases, such as beam–column joints, were also tested with ECC, showing a modest improvement in joint ductility with beams having a low aspect ratio ($a/d=2.5$). Shear cracks resulted in normal concrete, and more ductile flexural cracks were present in the ECC specimens with PVA fibers (Ismail *et al.* 2018).

Few studies have revised the performance of PVA fiber in specimens that incorporate typically large aggregates. Holschemacher and Höer (2008) investigated the use of PVA with regular-sized aggregates (16 mm) under bending and single fiber pull-out tests, concluding that the addition of PVA fiber is beneficial in terms of ductility and load-carrying capacity. However, the results cannot be extended to structural elements easily. Hossain *et al.* (2013) investigated the influence of PVA fiber on the concrete matrix, observing that the addition of PVA fiber did not modify the

compressive strength substantially, analogous to ECC mixes (Ayub *et al.* 2019). Other research studies obtained similar results (Khan and Ayub 2016, Wang *et al.* 2020, Kim *et al.* 1999), showing increases in ductility with slightly larger residual compressive strain. The use of lightweight aggregate as coarse material has shown an increase in compression and splitting tensile strength increase, more pronounced with the addition of PVA fibers than steel fibers (Rustamov *et al.* 2021). In the case of beam tests, the addition of PVA in concrete mixes with normal maximum aggregate size (20 mm) showed no relevant improvement in flexural strength but an increase in ductile post-cracking behavior (Shafiq *et al.* 2016). This result is consistent with the large improvement observed for high PVA fiber volume content (1–4%) of ECC specimens in tension, reaching 3% elongation before the initiation of strength degradation (Li and Li 2013).

At the structural level, for specimens with PVA and traditional reinforcement, the work by Jabbour *et al.* (2021) presented tests on short RC beams ($a/d=2.2$) with normal aggregate size (20 mm) and the addition of PVA fibers up to 1%. One of the short beams included stirrups, such that flexural behavior was promoted over shear behavior. Little differences were noted with the incorporation of PVA fibers, whereas the specimen without stirrups showed an improved ductility with a 30% larger deflection for 1% volume of PVA. The modest improvement might have been associated with the failure mode that presented important shear cracks in all cases. Similarly, the work by Meng *et al.* (2017) presented beams with and without stirrups, but for a larger a/d ratio (3.3). Their results showed a ductility improvement with the use of PVA in the specimen without stirrups compared to normal concrete. However, in this case, the specimens with PVA did not consider the large aggregate size. The use of PVA in shear walls has also shown ductility improvement (Zhang and Chen 2021).

This paper presents an experimental program on the behavior of concrete reinforced with PVA micro-fibers, varying the coarse aggregate size. The study aims to obtain stress-strain behavior in tension and compression and assess the behavior of FRC beams with PVA. The testing included 60 concrete cylinders in compression, 18 concrete cylinders in direct tension, 42 disks in indirect tension, and 12 beams under flexural loading to capture the tensile concrete capacity. Additionally, eight beams with traditional steel reinforcement were tested to observe the impact of PVA in slender and short structural elements, where limited information was available in the literature. In particular, failure modes and displacement capacities are studied, which are fundamental aspects to consider in element design.

2. Experimental program

The following section details the characteristics of the experimental program, the materials and the PVA-FRC mixture used in the experimental tests, and the tests used to characterize the material and structural response. The materials used to produce the three different mixtures included ASTM type IP portland-pozzolan cement, fine aggregate (sand) with No. 4 nominal maximum size, coarse aggregate (angular gravel) with 12 mm nominal maximum size, superplasticizer, and tap water.

2.1 PVA fibers

Three types of KURALON™ PVA fibers, referred to as A, B, and C, as shown in Fig. 1, were used in this investigation. Oil-coated PVA fibers, 12 mm and 15 mm long, were tested with fine-



Fig. 1 – KURALON™ PVA fibers used in the study: (a) A, (b) B, and (c) C

Table 1 Properties of the materials used in the mixture

Fiber	Fiber's Notation	Specific gravity (g/cm ³)	Diameter (μm)	Length (mm)	Tensile strength (MPa)	Young's modulus (GPa)	Elongation (%)
A	REC 15/12 mm	1.29	40	12	1560	41	6.5
B	RECS 100L/12 mm	1.29	100	12	1200	28	12.5
C	RF 600/15 mm	1.29	240	15	1495	42	7.5

Table 2 Mixture proportions

Mixture name	Tag	Maximum aggregate size (mm)	Cement content (kg/m ³)	Water content (kg/m ³)	Sand-to-total ratio	Aggregate (kg/m ³)		
						Gravel	Sand	
							Coarse	Fine
Gravel	GA	12.5	796	318	0.525	980	637	477
Coarse sand	CSA	4.75	796	318	1	0	1197	897
Fine sand	FSA	0.475	796	318	1	0	0	2094

and coarse-aggregate concrete specimens. The mechanical properties of the fibers are shown in Table 1. The KURALON™ REC 15/12 mm is denoted as fiber A, RECS 100L/12 mm as fiber B, and RF 600/15 mm as fiber C.

2.2 Mixture

The primary consideration when developing the aggregate proportions was the gradation of the final mix. A well-gradated curve indicates the mixture can hold particles of a broad range of sizes, with a good representation of particle sizes from the No. 4 to 200 sieves. Table 2 lists the aggregate amounts used in each mixture and the tag assigned to each mixture, and Fig. 2 depicts the sieve analysis performed for each mixture.

Two groups of specimens were cast, maintaining the distribution of aggregate but varying the other components. For group 1, three specimens were cast for each mixture, although only two specimens were tested, and the other specimen was cut into three disks to perform the indirect tensile test. In this group, all three fiber types were used. Fiber A was used in the coarse aggregate

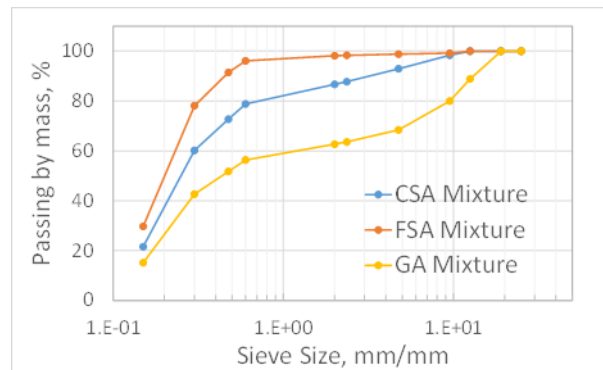


Fig. 2 – Sieve Analysis for GA, CSA and FSA mixtures

Table 3 Mixture testing matrix

Group	Fiber type	Aggregate type	PVA content (%)
1	A	GA	0, 0.62, 1.23
		GA	0, 0.62, 1.23
	B	CSA	0, 0.62, 1.23
		FSA	0, 0.62, 1.23
	C	GA	0, 0.62, 1.23
		CSA	0, 0.62, 1.23
2	A	FSA	0, 0.62, 1.23
		GA	0, 1.23, 2
		CSA	0, 1.23, 2
		FSA	0, 1.23, 2

mixture (GA), and all three mixtures included the remaining fibers (B and C), i.e., coarse aggregate (GA), coarse sand (CSA), and fine sand (FSA). All mixtures had a water-to-cement ratio w/c of 0.4. The fiber content of the three mixtures in each group was 0%, 0.62%, and 1.23%, which was added to the mixture during the cement paste mixing process. The matrix detail is shown in Table 3. In the case of group 1, the structural beam tests focused on the mixtures with amounts of PVA of 0% and 1.23%. This group was included to make a selection of a fiber type for future studies.

Group 2 was incorporated using only fiber A, with some variations to w/c and time to maturity, adding a higher content of PVA fiber (2%). For this group, direct tensile and beam tests were carried out on all aggregate types, while the structural beam tests focused on the mixtures with amounts of PVA of 0% and 2%. The amount of water was initially the same for all the mixtures ($w/c = 0.45$), but it was later decided to increase w/c to 0.51 in the CSA and FSA mixtures because of workability issues, especially when adding the fibers. In addition, the amount of superplasticizer (1500 ml/m³) and cement (796 kg/m³) added to the water was the same for all mixtures and groups. The zero-fiber content in this group was considered in order to have a control group, although there are small differences in w/c and maturity time with group 1.

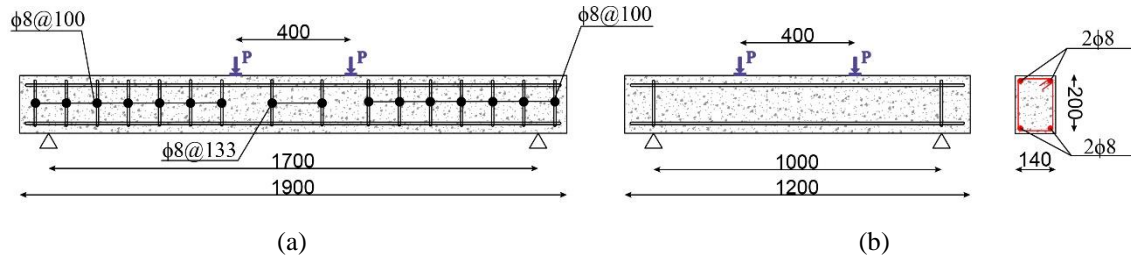


Fig. 3 – Beam details: (a) slender specimen and (b) short specimen (units in mm)

2.3 Steel reinforcement

The steel used in this research was A630-420H steel, with a nominal tensile strength of 630 MPa and yield strength of 420 MPa. Tensile tests were performed on the 8-mm diameter bars ($\phi 8$ bars) used in the structural beam test. The actual yield stress was 564 MPa on average, and the maximum stress was 774 MPa on average.

2.4. Structural beam tests

Eight structural beams were tested to assess the influence of fiber content on both flexural and shear behavior. Four were slender beams and intended to fail in flexure (Fig. 3(a)), and the other four were short beams meant to fail in shear (Fig. 3(b)). All beams were assembled using $\phi 8$ A630-420H steel bars as stirrups and longitudinal reinforcement rebars. Just two mixtures were used for all beams: GA concrete with 1.23% PVA with fiber A for group 1, and the PVA content was increased to 2% for group 2. The slender beams were 1900 mm long with a cross-section of 140×200 mm, supported on two simple supports spaced at 1700 mm. The short beams were 1200 mm long with the same cross-section, simply supported on both ends separated by 1000 mm. Both types of beams had two longitudinal $\phi 8$ steel rebars at the bottom and two $\phi 8$ steel rebars at the top. The slender beams met the tensile and shear minimum reinforcement ratio according to ACI 318 (2019), but the short beams did not, owing to the lack of stirrups, representing the potential behavior of slabs.

The load P was applied at two points on each specimen using a rigid beam, 200 mm from the center, monotonically incremented. The nominal flexural capacity of the slender specimen is reached for a transverse load of 30 kN. However, the short specimen yielded a load of 65 kN, whereas the nominal shear capacity of concrete is reached for a transverse load of 50 kN, indicating that flexural failure would be expected for the slender specimen and shear failure for the short specimen. A load cell measured the applied load, and a non-contact technique called Digital Image Correlation (DIC) was employed to measure element deformation. DIC uses image registration algorithms to track the relative displacements of element points between a reference image and a current image, undeformed and deformed images, respectively (Blaber *et al.* 2015).

3. Test results

A series of compressive and tensile (direct, indirect, and bending) tests were performed to

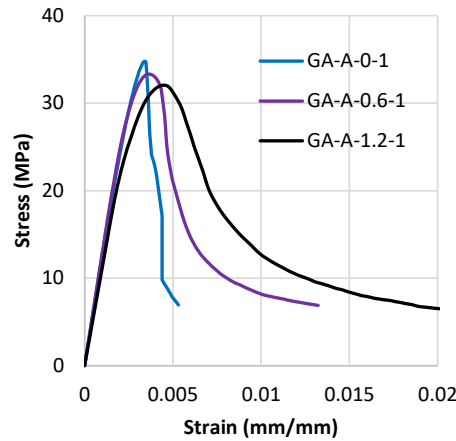


Fig. 4 – Compression test results for Group 1, fiber A and GA

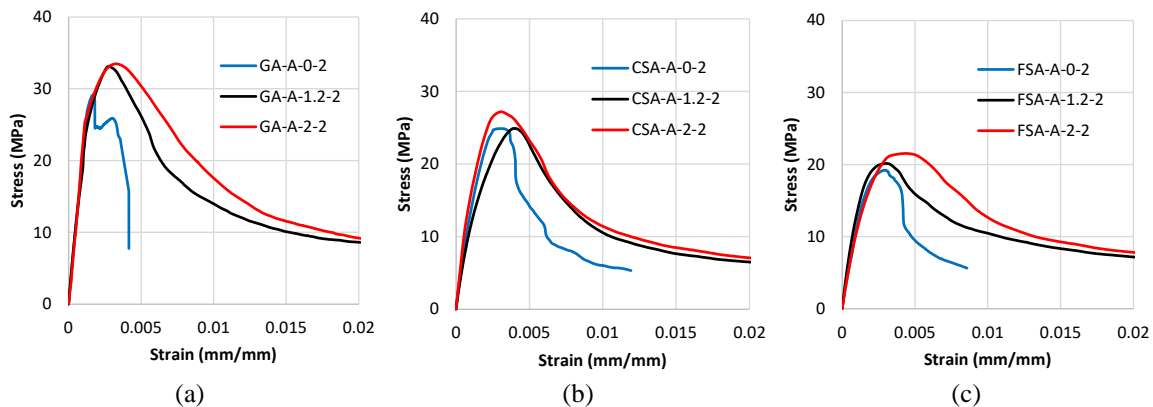


Fig. 5 – Compression test results for different fibers and aggregate for Group 2 with fiber A: (a) GA, (b) CSA, and (c) FSA

characterize the material properties. For compression, specimens from groups 1 and 2 were tested, whereas only specimens from group 1 were assessed with indirect tensile tests. Additionally, direct tensile and bending tests were performed on the specimens from group 2. For all mixtures, twin specimens were tested, and their average results are reported. Each specimen was cast and cured for approximately 50 days for group 1 and about 200 days for group 2. Additionally, eight structural beams under bending were tested to evaluate the flexural and shear responses for cases with and without fibers.

3.1 Compression tests

Specimens 100 mm in diameter and 200 mm in height were tested at a deformation rate of 0.5 mm/min. Each specimen was tested until an 80% strength degradation was reached. A universal testing machine load cell recorded the load, and the deformation was assessed by two opposing LVDTs attached to the specimens by an external ring suspended on the specimen surface. Both

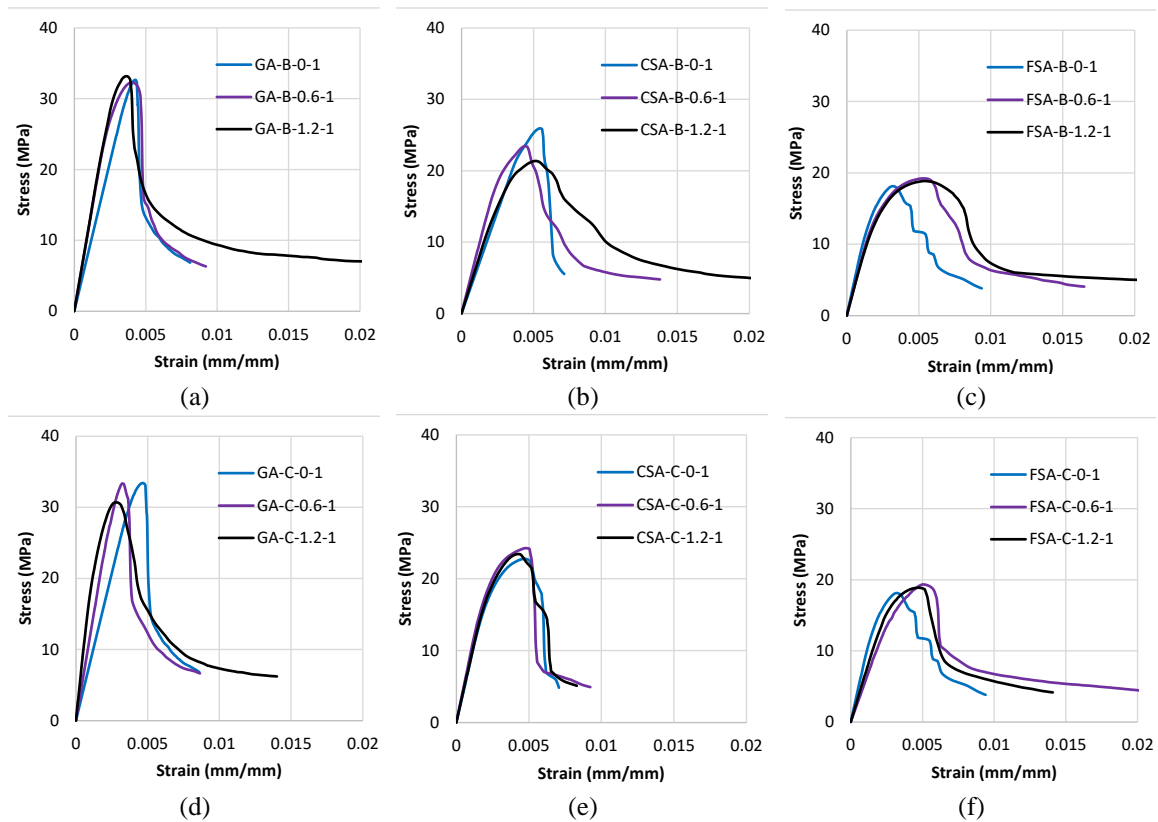


Fig. 6 – Compression test results for different fibers and aggregate for group 1 with (a-c) fibers B and (d-f) C, and aggregates (a, d) GA, (b, e) CSA, and (c, f) FSA

LVDTs could assess the specimen strain before the peak strength. However, after the peak, the rings would loosen, and the internal measurement from the universal testing machine was used instead. To present the results, an average from the two curves from companion specimens for each mixture was calculated.

The compression testing results are summarized for the different mixtures in Figs. 4, 5 and 6. Each subfigure compares the response of each fiber, varying its fiber content by color, blue, purple, black, and red are 0%, 0.62%, 1.23%, and 2% fiber content, respectively. Given that 2% fiber content was only used for group 2, it is shown in selected subfigures. The plain concrete specimens exhibited a fragile response after the peak stress (blue curve on each graph), having an abrupt stress decrease. On the other hand, specimens with different fiber content showed lower stress-decreasing rates after the stress peaks, in other words, those specimens had more ductile failure presenting a residual strength after the peak. Fig. 4 shows another particularity. Due to the addition of PVA fiber to the mixture, as the PVA amount increases, its compressive capacity decays. This is because PVA fibers tend to produce air voids inside the mixture, more PVA means more air voids, which does not help to increase the stress capacity. This phenomenon is consistent with researchers' work on PVA fiber investigation with mortars.

However, such ductility increase was typical for fiber A (the reason for its selection in group 2), as shown in Figs. 4 and 5(a-c), and less evident for fibers B and C, given their smaller aspect

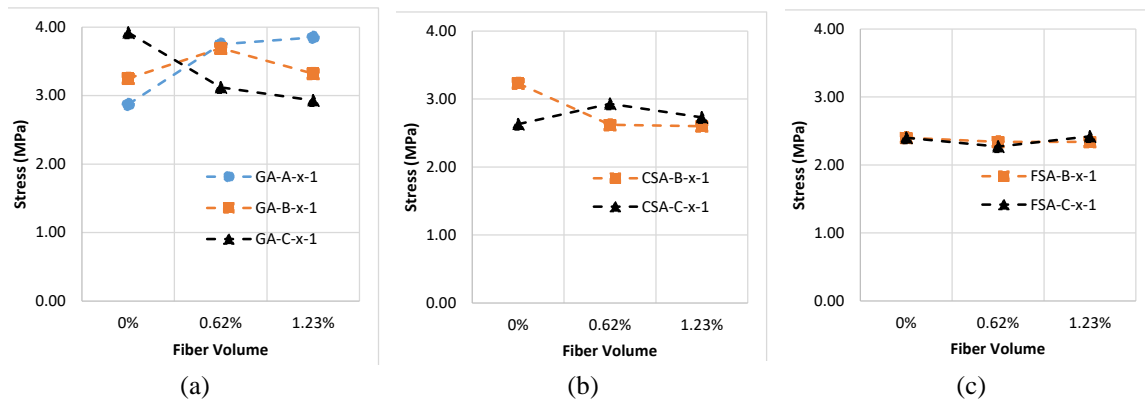


Fig. 7 – Indirect tension strength for mixtures with aggregates: (a) GA, (b) CSA, and (c) FSA

ratios (Table 1). A strength reduction of 50% with fiber A was observed at compressive strains of about 1% for 1.23% fiber content. The ductility improvement by increasing the fiber content from 1.23% to 2% was small. The specimens with fibers B and C showed an increase in ductility with mixes having the smallest aggregate content size (FSA) in Fig. 6(c, f), as observed in the ECC. In GA, almost no difference was noted with the use of such fibers, as shown in Fig. 6(a, d). In a few cases, the addition of fiber caused a moderate reduction in compressive strength. The largest reduction was observed by modifying the aggregate type, with a ratio close to 1:0.7:0.6 for GA, CSA, and FSA, respectively, and mostly independent of the fiber type (Fig. 5, 6).

3.2 Indirect tensile test

Indirect tensile tests, or splitting tests, were performed on both plain concrete and PVA-fiber concrete disks, similar to the testing by Hamoush *et al.* (2010). These disks were 100 mm in diameter and 50 mm in width to obtain a dimension ratio of 1:2. Testing was performed by a universal testing machine, with displacement control at 1 mm/min. The indirect tensile test was only used to measure each specimen's maximum tensile capacity. Fig. 7 shows the maximum tensile strength of the different mixtures tested for group 1 (average of two identical specimens), and each plot compares the response for the different aggregate sizes. Fig. 7 shows that, in general, small differences in the maximum stress capacity occurred between comparable specimens. Specimens with fibers B and C presented almost no strength variation for FSA, as shown in Fig. 7(c). On the other hand, Fig. 7(a) shows that the use of fiber A and the GA mixture yielded an improvement in the tensile strength with the increase of fiber content.

3.3 Direct tension tests

Studies have shown that the direct tensile testing method is a more reliable way to assess the concrete tensile strength than the splitting tensile and bending testing methods (Swaddiwudhipong *et al.* 2003, Choi *et al.* 2014). Nonetheless, it is a difficult test to perform in the laboratory because of the bonding material used to glue the specimen to the testing machine. Furthermore, the torsional action generated while the testing machine accommodates the eccentric loading can cause issues. Dog bone-shaped specimens have been used to avoid these problems, but given the

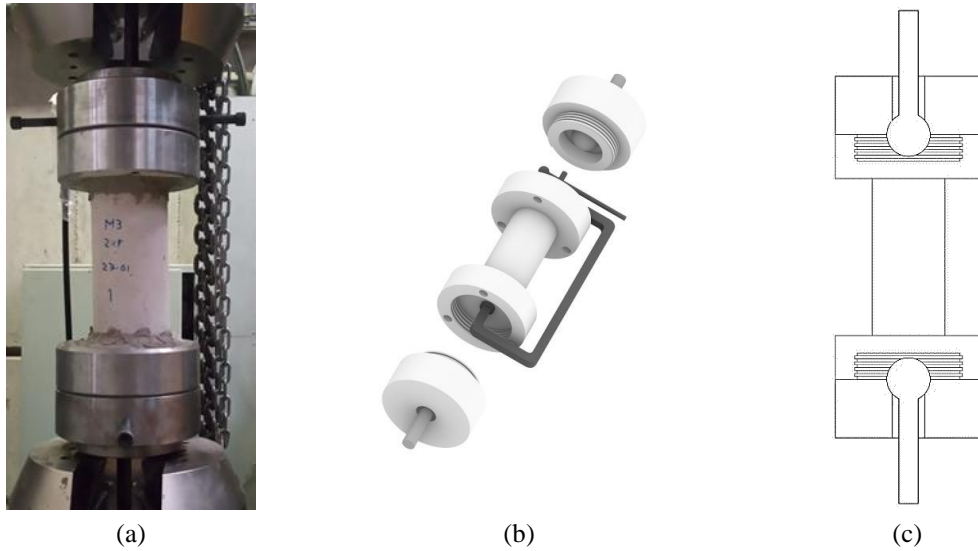


Fig. 8 – Direct tensile testing equipment: (a) setup, (b) 3D view, and (c) 2D sectional view

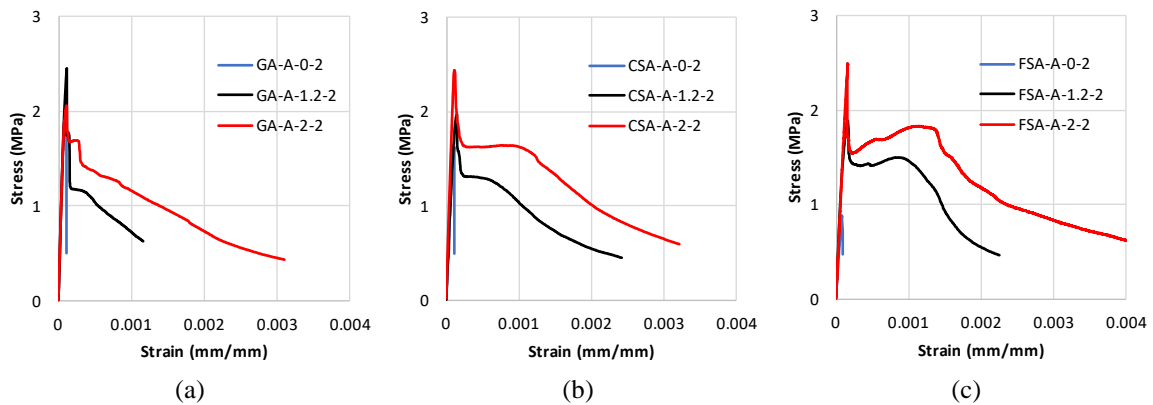


Fig. 9 – Direct tensile stress vs. strain curves: (a) GA, (b) CSA, and (c) FSA

dimensions of the specimens and the fibers, the results in the literature showed significant differences, where the peak tensile strengths and strain capacities of cylindrical specimens were lower than those of the dog-bone specimens (Yu *et al.* 2018, Mechtcherine *et al.* 2011). This response difference could be attributed to three factors: the geometry-induced difference in tensile properties, i.e., the variations in initial imperfections (such as air voids and shrinkage cracks), fiber dispersion and alignment, and the border conditions (Yu *et al.* 2018).

To avoid the aforementioned limitations for dog-bone specimens, tensile tests were performed with cylinders. Special equipment was designed to avoid unintended torsion while closing/tightening the clamps that attach the specimen to the testing machine, which was observed in previous tests. The tensile device consists of three main pieces that are assembled into the universal testing machine. The equipment employs circular metal plates that are adhered to both sides of the test piece and supported by the clamps of the machine through a cylindrical bar that

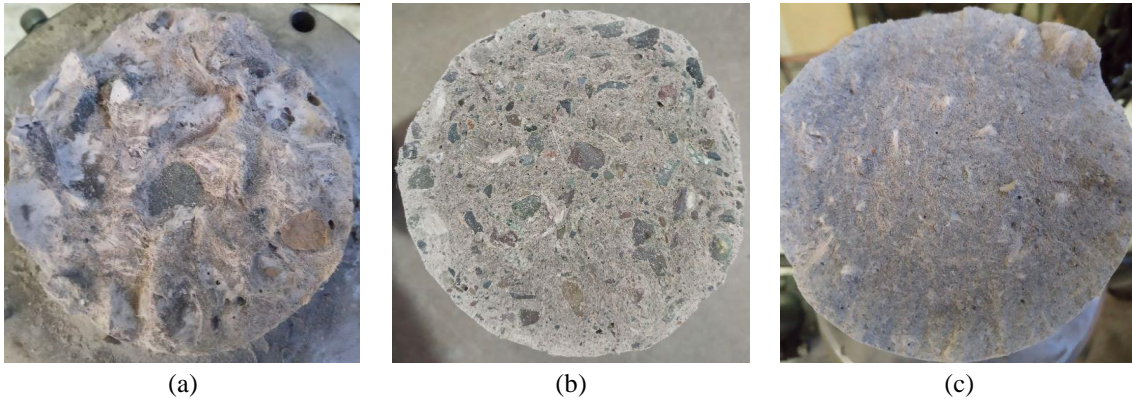


Fig. 10 – Fiber and aggregate distribution within the matrix: (a) GA, (b) CSA, and (c) FSA

protrudes from the plates (Fig. 8). In this device, the torsional action is eliminated by the universal ball joint that connects to the clamp.

The tensile tests were carried out on specimens 100 mm in diameter and 200 mm in height at a speed of 0.5 mm/min, with the universal machine programmed to end the test when the load decreased to 20% of the maximum load. For the stress-strain curve, the data from the LVDT sensors were used for the pre-cracking stage, and the data obtained from the universal machine was used for the post-cracking stage to avoid spurious data caused by local damage where the sensors were located. Fig. 9 shows the stress versus strain response for all three mixtures, with data averaged from twin specimens. In the case of FSA with 2% fiber volume, the data from only one specimen (instead of averaging twin specimens) is shown given testing problems with the twin specimen.

In general, an increase of peak tensile stress occurred with the addition of fibers, which, in the case of CSA, was about twice the strength without fiber, reaching similar values as for the other mixes with fibers. The ductility of each of the three types of mixtures increased with the volume of the fiber, exhibiting degradation to a stress level of about 0.5 MPa with a strain above 0.1% for 1.23% fiber volume and above 0.2% for 2% fiber volume. In the case of the smallest aggregate size (FSA), the fiber content increased the toughness to a larger extent than with the other mixes, as is commonly observed with ECC.

Fig. 10 shows the distribution of aggregate and fibers for each type of mixture, where a more uniform distribution was seen for FSA, given the smaller aggregate size in Fig. 10(c). The larger aggregate size for GA in Fig. 10(a) resulted in the clustering of fibers since the granular material occupied a greater space, preventing a uniform distribution of the fiber in the specimen.

3.4 Bending tests

In the bending test of the prismatic specimens, the arrangement of the loads considered two identical load points separated by 150 mm with a test span of 500 mm. Similar to the previous tests, the speed was set to 0.5 mm/min, ending after a decay of 80% of the maximum load. Fig. 11 shows the curves of load versus central transversal displacement, where similarly to the other cases, the data extracted from the LVDT sensors (mounted on the specimens) was used for the pre-cracking stage, and the data from the testing equipment (piston) was used in the post-cracking

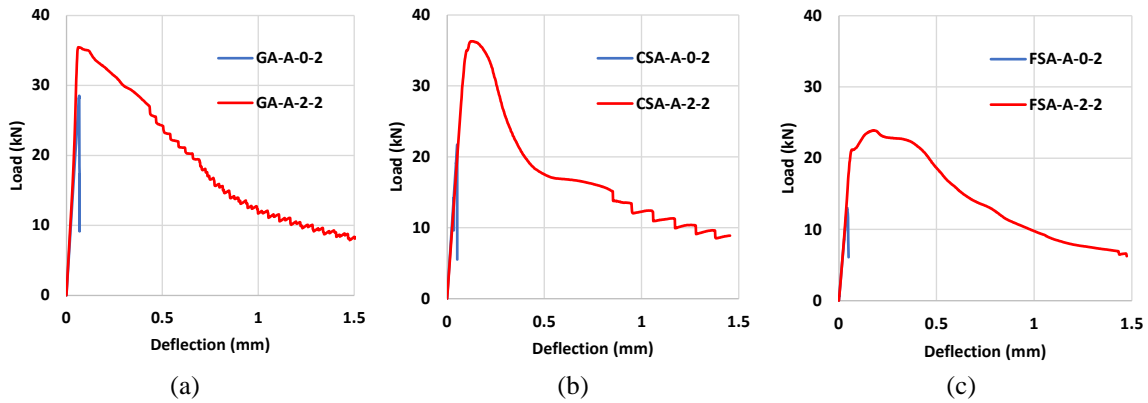


Fig. 11 – Bending test response (group 2): (a) GA, (b) CSA, and (c) FSA

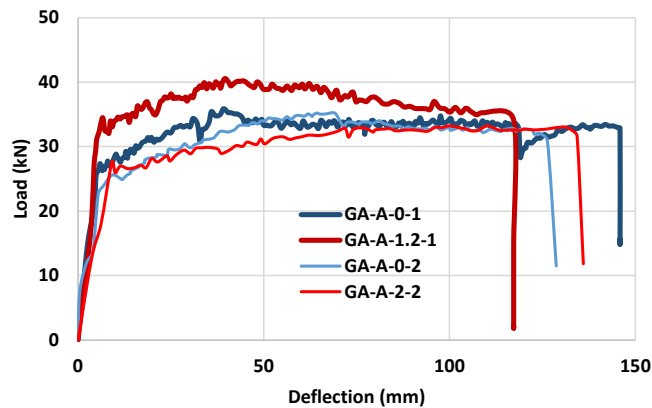


Fig. 12 – Bending test of slender beam for both groups

response. This approach avoids alterations to the LVDT reading with concrete debris that could fall from the specimen during the damaging process. The average data from twin specimens are presented for all mixtures.

According to Fig. 11, an increase in the strength in the specimens with fibers was observed, especially for CSA and FSA, where increases of 60% and 85%, respectively, were obtained on average compared with specimens with plain concrete. In the case of GA, the increase was lower (15%), but the addition of PVA fiber (2%) promoted a more ductile response, resulting in a curve similar to that of CSA. A ductile response was also observed in terms of deflection, without a significant difference among the mixtures. However, a reduced strength of FSA was noted, reaching about 1 mm of deflection for a 50% strength reduction for the specimens with fibers, whereas the specimens without fibers presented an abrupt strength drop after reaching the peak load. This response is consistent with the observation of specimens under the direct tension test.

3.5 Structural bending test

To evaluate the effect of PVA fibers in RC beam specimens, slender and short beams were considered to capture flexural and shear failure mechanisms. The largest aggregate size (GA) was

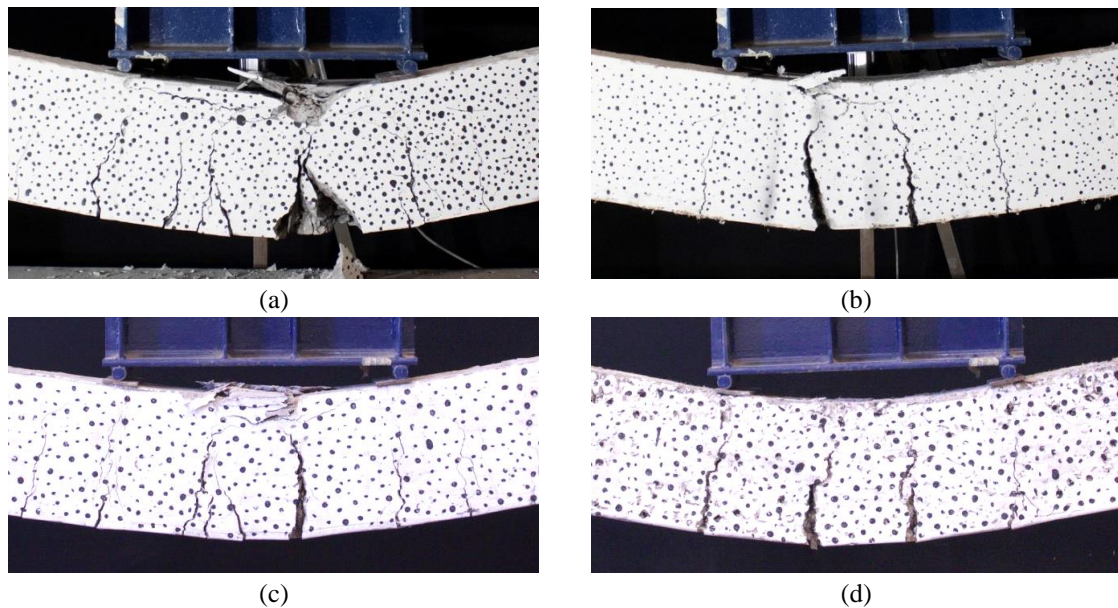


Fig. 13 – Slender beam failure: (a) 0% fiber, group 1, (b) 1.23% fiber, group 1, (c) 0% fiber, group 2, and (d) 2% fiber, group 2

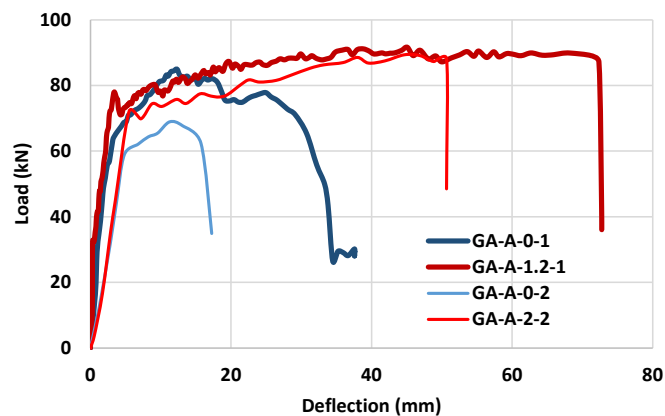


Fig. 14 – Bending test of short beam for both groups

used to observe its impact at the structural level, and fiber A was considered, which presented better performance during the material characterization (ductility increase).

3.5.1 Slender beams

Fig. 12 shows the load versus deflection response of the slender beams. The beams with 1.23% and 0% PVA content from group 1 had peak load capacities of about 41 and 36 kN, respectively. In this particular case, the specimen with PVA fiber showed a higher load capacity than the plain concrete beam, but the displacement capacity was slightly lower than that of the control beam. Despite this moderate difference, a large ductility was observed in both cases. For group 2, both beams showed similar behavior. Maximum loads of 35 and 33 kN were obtained for the beam 0% and 2% fiber, respectively, showing a moderate strength reduction but with similar magnitudes as

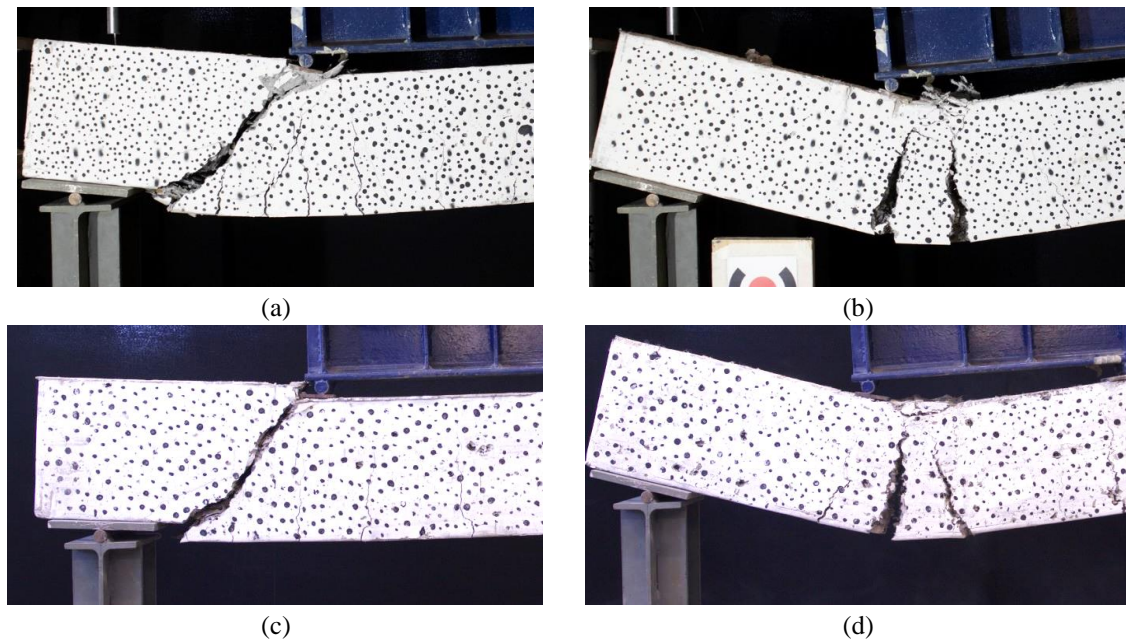


Fig. 15 – Short beam failure: (a) 0% fiber, group 1, (b) 1.23% fiber, group 1, (c) 0% fiber, group 2, and (d) 2% fiber, group 2

with group 1. The maximum deflections were almost equal, which is comparable with the specimen without fiber from group 1. Thus, the addition of fiber did not improve the flexural behavior of the beam even though the steel reinforcement ratio (0.4%) was almost the minimum required for beams according to ACI 318-19 (2019).

Fig. 13 depicts the failure mode for each slender beam. Large cracks were observed at the ultimate stage once strength degradation was set, with similar distribution for all cases. The initiation of concrete spalling could also be observed in the upper section of the specimens.

3.5.2 Short beams

Fig. 14 shows the load versus deflection response of the short beams. The beams with 1.23% and 0% PVA-fiber content from group 1 had peak load capacities of about 92 and 85 kN, respectively. The beam with PVA fiber showed a higher load capacity and a larger deflection, double the maximum deflection observed in the plain concrete beam. In the case of group 2, the short beams reached peak loads of 69 and 89 kN for the plain specimen and the specimen with 2% fiber volume, respectively. A 30% strength increase occurred, larger than in the case of group 1, along with almost three times the deflection capacity observed with the plain concrete case. The deflection increase with fiber is associated with a modification of the failure mode.

Fig. 15 shows the failure mode for each short beam tested. Each beam, with and without fibers, had a different failure mode. The beams with 0% PVA content (both groups) presented shear cracks due to the lack of stirrups, as it can occur in foundations and slabs. However, both specimens with PVA fibers from groups 1 and 2 (1.23% and 2% PVA content) changed their failure mode into flexural, exhibiting large vertical cracks in the central portion of the beams. This

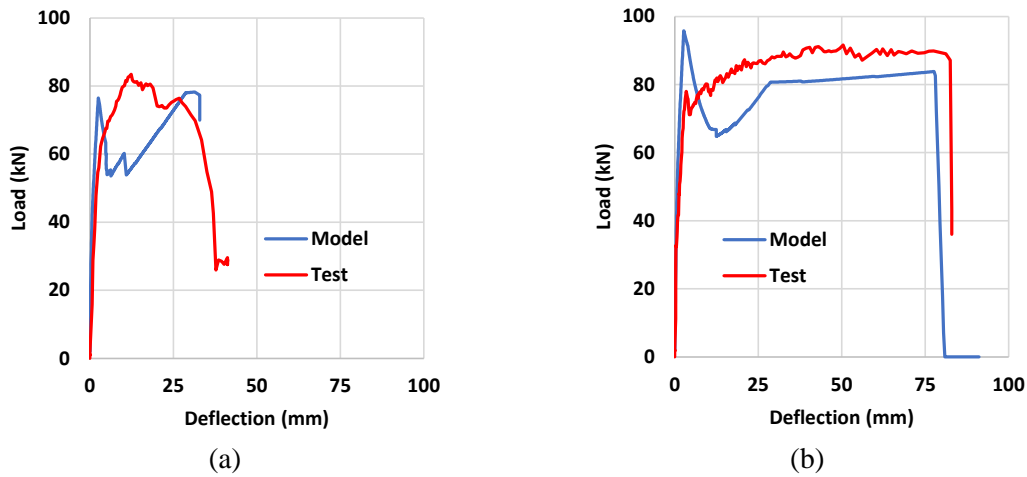


Fig. 16 – Model result comparison of group 1 short beams: (a) GA-A-0-1 and (b) GA-A-1.2-1

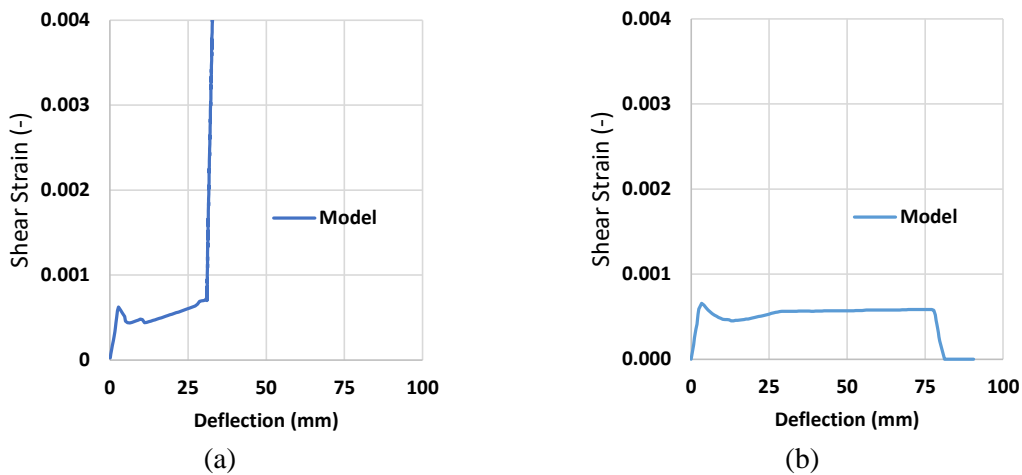


Fig. 17 – Model shear strain (ϵ_{xy}) of group 1 short beams: (a) GA-A-0-1 and (b) GA-A-1.2-1

is a desirable behavioral improvement, preventing shear failure by promoting a more ductile flexural response.

The results of the testing indicate that the incorporation of PVA fibers, in particular, fiber type A, for concrete mixes that include large aggregate size (GA) is beneficial to the concrete's tensile ductility, improving the structural behavior and avoiding a fragile shear failure, which is common in elements without shear reinforcement. This can also impact design since the assessment of displacement capacity in structural elements has become more common with the ascent of performance-based design, where displacement demands are translated into potential flexural damage as curvature or strain demands (Massone and Cáceres 2020, Massone and Alfaro 2016).

A computational analytical model was assembled to replicate the short beam pushover behavior observed in the laboratory. The pushover analytical model was performed using the E-SFI model (Massone *et al.* 2021, López *et al.* 2022) in the platform OpenSees. It is a column-type model with 3 degrees of freedom at each end node (for 2D analysis), assuming the Bernoulli hypothesis and

perfect adherence between concrete and steel. The section is discretized in panel elements using a fixed-angle material model (Orakcal *et al.* 2019) with steel and concrete embedded. The uniaxial constitutive laws for concrete and steel, required for the panel formulation used in the model, were determined based on the tested properties. This fiber-type model is capable of capturing the shear behavior, thus, it is ideal for analysis, especially for the short beams.

The analytical results compared with the experimental short beam specimens, for group 1, are shown in Fig. 16. The short beam with 0% fiber model (Fig 16a) presents a slightly lower loading and deflection capacity compared with the test. With the addition of fibers (Fig. 16b), the loading capacity increases modestly, but the deflection capacity increases considerably (about twice), which is observed consistently in the model and the test. In order to understand the differences in behavior, Fig. 17 depicts the shear strain (ϵ_{xy}) of both short beam models for the most deformed panel element. For the short beam with 0% fiber (Fig. 17a), the shear strain drastically increases at the end of the analysis compared to the case with PVA fibers, indicating damage localization due to shear failure in the specimen without fibers. For the specimen with PVA fibers, the shear strains are similar once the peak loading is reached, but they decrease as the strength drops, which indicates that the failure mode is not associated with shear, but rather flexure.

4. Conclusions

This investigation characterizes the influence of PVA-fiber content up to 2% with coarse aggregate in the concrete matrix. The testing showed that the addition of fibers did not have a significant impact on the compressive strength, where the largest strength was observed with the large aggregate size (GA), with a strength reduction of less than 10% for 1.2% fiber volume. However, the PVA fibers increased the post-peak stress, yielding a more ductile response. Moreover, such response was superior for fiber A, which presented a higher aspect ratio than the other two fibers, especially when combined with GA.

Indirect tensile tests showed that increasing the PVA content increased the tensile strength for GA with fiber A, which was not reproduced for the other fiber types. The other aggregates presented little variation in tensile strength. In the case of direct tensile tests, although the smaller aggregate-size specimens (CSA and FSA) presented larger improvements in strength with the use of fiber, a similar ductile response was observed with the addition of fibers in all aggregate-size cases. Such ductile response was also evident in the concrete beam specimens under bending, with an improvement of 16% in strength (combined with fiber A).

From the short RC beams specimens, the failure modification was noticeable when adding PVA fiber to the mixture. PVA incorporation switched the failure mode to flexure with a ductile response. Beams with PVA presented improvements in strength but, more significantly, increases in ductility, up to three times larger deflection levels when compared with the control beam. On the other hand, the slender RC beams presented similar results, with little variation in response and identical failure mode. Thus, the incorporation of PVA fibers, in particular, fiber type A, in concrete mixes that include large aggregate size (GA) has a beneficial impact on elements susceptible to shear failure, such as structures without transverse reinforcement.

A model was used to predict the response for the short structural beam elements. The model can capture the switched failure mode between the specimen reinforced with PVA and the specimen without fibers presenting a reduction of deflection capacity in the case without fibers, which is associated with an increase in shear strains consistent with shear failure.

Acknowledgments

This work was funded by the National Agency for Research and Development (ANID) for the project Fondecyt Regular 2020 N°1200023. The authors would like to also thank the support of Mr. Pedro Soto for his help with the laboratory setup and testing.

References

- ACI 318-19, American Concrete Institute (2019), “Building code requirements for structural concrete and commentary”, Farmington Hills, Mich.
- Aghdasi, P., Heid, A.E. and Chao, S.H. (2016), “Developing ultra-high-performance fiber-reinforced concrete for large-scale structural applications”, *ACI Mater. J.*, **113**(5), 559-570. <https://doi.org/10.14359/51689103>.
- Alyousif, A., Anil, O., Sahmaran, M., Lachemi, M., Yildirim, G., Ashour, A.F. (2016), “Comparison of shear behaviour of engineered cementitious composite and normal concrete beams with different shear span lengths”, *Magazine Concr. Res.*, **68**(5), 217-228. <https://doi.org/10.1680/jmacr.14.00336>.
- Ayub, T., Khan, S.U., Ayub, A. (2019), “Analytical model for the compressive stress-strain behavior of PVA-FRC”, *Constr. Build. Mater.*, **214**, 581-593. <https://doi.org/10.1016/j.conbuildmat.2019.04.126>.
- Batran, T.Z., Ismail, M.K., Hassan, A.A.A. (2021), “Flexural behavior of lightweight self-consolidating concrete beams strengthened with engineered cementitious composite”, *ACI Mater. J.*, **118**(4), 39-50. <https://doi.org/10.14359/51732635>.
- Blaber, J., Adair, B. and Antoniou, A. (2015), “Ncorr: Open-source 2D digital image correlation matlab software”, *Exp. Mech.*, **55**(6), 1105-1122. <https://doi.org/10.1007/s11340-015-0009-1>.
- Brandt, A.M. (2008), “Fibre reinforced cement-based (FRC) composites after over 40 years of development in building and civil engineering”, *Compos. Struct.*, **86**(1-3), 3-9. <https://doi.org/10.1016/j.compstruct.2008.03.006>.
- Cao, M., Li, L., Shen, S. (2019), “Influence of reinforcing index on rheology of fiber-reinforced mortar”, *ACI Mater. J.*, **116**(6), 95-105. <https://doi.org/10.14359/51716816>.
- Choi, S.J., Yang, K.H., Sim, J.I. and Choi, B.J. (2014), “Direct tensile strength of lightweight concrete with different specimen depths and aggregate sizes”, *Constr. Build. Mater.*, **63**, 132-141. <https://doi.org/10.1016/j.conbuildmat.2014.04.055>.
- Georgiou, A.V. and Pantazopoulou, S.J. (2019), “Experimental and analytical investigation of the shear behavior of strain hardening cementitious composites”, *Struct. Eng. Mech.*, **72**(1), 781-792. <https://doi.org/10.12989/sem.2019.72.1.019>.
- Hamoush, S., Abu-Lebdeh, T. and Cummins, T. (2010), “Deflection behavior of concrete beams reinforced with PVA micro-fibers”, *Constr. Build. Mater.*, **24**(11), 2285-2293. <https://doi.org/10.1016/j.conbuildmat.2010.04.027>.
- Holschemacher, K. and Höer, S. (2008), “Influence of pva fibers on load carrying capacity of concrete with coarse aggregates”, *In 7th Int. Rilem Symp. on Fibre Reinforced Concrete: Design and Applications*, 219-229.
- Horikoshi, T., Ogawa, A., Saito, T., Hoshiro, H., Fischer, G. and Li, V. (2006), “Properties of polyvinyl alcohol fiber as reinforcing materials for cementitious composites”, *Proceedings of the International RILEM Workshop on High Performance Fiber Reinforced Cementitious Composites in Structural Applications*, 145-153.
- Hossain, K.M., Lachemi, M., Sasmour, M. and Sonebi, M. (2013), “Strength and fracture energy characteristics of self-consolidating concrete incorporating polyvinyl alcohol, steel and hybrid fibres”, *Construction and Building Materials*, **45**, 20-29. <https://doi.org/10.1016/j.conbuildmat.2013.03.054>.
- Ismail, M.K., Abdelaleem, B.H., Hassan, A.A.A. (2018), “Effect of fiber type on the behavior of cementitious composite beam-column joints under reversed cyclic loading”, *Constr. Build. Mater.*, **186**,

- 969-977. <https://doi.org/10.1016/j.conbuildmat.2018.08.024>.
- Jabbour, R., Assaad J.J., Hamad, B. (2021), "Cost-to-performance assessment of polyvinyl alcohol fibers in concrete structures", *Mech. Adv. Mater. Struct.*, **29**(20), 2973-2983. <https://doi.org/10.1080/15376494.2021.1882625>.
- Kang, T.H.K., Kim, W., Massone, L.M., Galleguillos, T.A. (2012), "Shear-flexure coupling behavior of steel fiber-reinforced concrete beams", *ACI Struct. J.*, **109**(4), 435-444. <https://doi.org/10.14359/51683863>.
- Karimpour, H., Mazloom, M. (2022), "Pseudo-strain hardening and mechanical properties of green cementitious composites containing polypropylene fibers", *Struct. Eng. Mech.*, **81**(5), 575-589. <https://doi.org/10.12989/sem.2022.81.5.575>.
- Khan, S.U. and Ayub, T. (2016), "Modelling of the pre and post-cracking response of the PVA fibre reinforced concrete subjected to direct tension", *Constr. Build. Mater.*, **120**, 540-557. <https://doi.org/10.1016/j.conbuildmat.2016.05.130>.
- Kim, J.H., Robertson, R.E., Naaman, A.E. (1999), "Structure and properties of poly(vinyl alcohol)-modified mortar and concrete", *Cement Concr. Res.*, **29**, 407-415. [https://doi.org/10.1016/S0008-8846\(98\)00246-4](https://doi.org/10.1016/S0008-8846(98)00246-4).
- Li, M., Li, V.C. (2013), "Rheology, fiber dispersion, and robust properties of engineered cementitious composites", *Mater. Struct.*, **46**, 405-420. <https://doi.org/10.1617/s11527-012-9909-z>.
- Li, Z., Li, F., Chang, T.Y.P. and Mai, Y.W. (1998), "Uniaxial tensile behavior of concrete reinforced with randomly distributed short fibers", *ACI Mater. J.*, **95**(5), 564-574. <https://doi.org/10.14359/399>.
- Massone L.M. (2013), "Fundamental principles of the reinforced concrete design code changes in Chile following the Mw 8.8 earthquake In 2010", *Eng. Struct.*, **56**, 1335-1345. <https://doi.org/10.1016/j.engstruct.2013.07.013>.
- López, C. N., Massone, L. M., Kolozvari, K. (2022), "Validation of an efficient shear-flexure interaction model for planar reinforced concrete walls", *Eng. Struct.*, **252**, 113590. <https://doi.org/10.1016/j.engstruct.2021.113590>.
- Massone, L. M., Aceituno, D., Carrillo, J. (2023), "Cumulative damage in RC frame buildings - The 2017 Mexico earthquake case", *Adv. Comput. Des.*, **8**(1), 15-38. <https://doi.org/10.12989/acd.2023.8.1.015>.
- Massone L.M., Alfaro J.I. (2016), "Displacement and curvature estimation for the design of reinforced concrete slender walls", *Struct. Des. Tall Spec. Build.*, **25**(16), 823-841. <https://doi.org/10.1002/tal.1285>.
- Massone, L.M., Cáceres, I. (2020), "Damage correlation in flexural walls with a displacement approach method for boundary detailing", *J. Build. Eng.*, **32**, 101807. <https://doi.org/10.1016/j.job.2020.101807>.
- Massone, L.M., Nazar, F. (2018), "Analytical and experimental evaluation of the use of fibers as partial reinforcement in shotcrete for tunnels in Chile", *Tunnel. Undergr. Sp. Technol.*, **77**, 13-25. <https://doi.org/10.1016/j.tust.2018.03.027>.
- Massone, L.M., López, C.N., Kolozvari, K. (2021), "Formulation of an efficient shear-flexure interaction model for planar reinforced concrete walls", *Eng. Struct.*, **243**, 12680. <https://doi.org/10.1016/j.engstruct.2021.112680>.
- Mechtcherine, V., Millon, O., Butler, M. and Thoma, K. (2011), "Mechanical behaviour of strain hardening cement-based composites under impact loading", *Cement Concr. Compos.*, **33**(1), 1-11. <https://doi.org/10.1016/j.cemconcomp.2010.09.018>.
- Meng, D., Lee, C.K., Zhang, Y.X. (2017), "Flexural and shear behaviours of plain and reinforced polyvinyl alcohol-engineered cementitious composite beams", *Eng. Struct.*, **151**, 261-272. <https://doi.org/10.1016/j.engstruct.2017.08.036>.
- Orakcal, K., Massone, L.M., Ulugtekin, D. (2019), "A constitutive model for reinforced concrete panel elements subjected to cyclic loading", *Int. J. Concr. Struct. Mater.*, **13**, 51. <https://doi.org/10.1186/s40069-019-0365-9>.
- Rustamov, S., Kim, S., Kwon, M., Kim, J. (2021), "Effects of fiber types and volume fraction on strength of lightweight concrete containing expanded clay", *Adv. Concr. Constr.*, **12**(1), 47-55. <https://doi.org/10.12989/acc.2021.12.1.047>.
- Sahmaran, M., Yücel, H.E., Demirhan, S., Arik, M.T. and Li, V.C. (2012), "Combined effect of aggregate and mineral admixtures on tensile ductility of engineered cementitious composites", *ACI Mater. J.*,

- 109**(6), 627-638. <https://doi.org/10.14359/51684160>.
- Shafiq, N., Ayub, T., Khan, S.U. (2016), "Investigating the performance of PVA and basalt fibre reinforced beams subjected to flexural action", *Compos. Struct.*, **153**, 30-41.
<https://doi.org/10.1016/j.compstruct.2016.06.008>.
- Shanour, A.S., Said, M., Arafa, A.I., Maher, A. (2018), "Flexural performance of concrete beams containing engineered cementitious composites", *Constr. Build. Mater.*, **180**, 23-34.
<https://doi.org/10.1016/j.conbuildmat.2018.05.238>.
- Swaddiwudhipong, S., Lu, H.R. and Wee, T.H. (2003), "Direct tension test and tensile strain capacity of concrete at early age", *Cement Concr. Res.*, **33**(12), 2077-2084.
[https://doi.org/10.1016/S0008-8846\(03\)00231-X](https://doi.org/10.1016/S0008-8846(03)00231-X).
- Thong, C.C., Teo, D.C. and Ng, C.K. (2016), "Application of polyvinyl alcohol (PVA) in cement-based composite materials: A review of its engineering properties and microstructure behavior", *Constr. Build. Mater.*, **107**, 172-180. <https://doi.org/10.1016/j.conbuildmat.2015.12.188>.
- Wang, Z., Zuo, J., Zhang, X., Jiang, G. and Feng, L. (2020), "Stress-strain behaviour of hybrid-fibre engineered cementitious composite in compression", *Adv. Cement Res.*, **32**(2), 53-65.
<https://doi.org/10.1680/jadcr.18.00072>.
- Yu, K., Li, L., Yu, J., Wang, Y., Ye, J. and Xu, Q.F. (2018), "Direct tensile properties of engineered cementitious composites: A review", *Constr. Build. Mater.*, **165**, 346-362.
<https://doi.org/10.1016/j.conbuildmat.2017.12.124>.
- Zhang, H.M., Chen, Z.Y. (2021), "Comparison and prediction of seismic performance for shear walls composed with fiber reinforced concrete", *Adv. Concr. Constr.*, **11**(2), 111-126.
<https://doi.org/10.12989/acc.2021.11.2.111>.